

# Wide or narrow? The phenomenology of 750 GeV diphotons

Matthew R. Buckley<sup>a</sup>

Department of Physics and Astronomy, Rutgers University, Piscataway, NJ 08854, USA

Received: 8 June 2016 / Accepted: 13 June 2016 / Published online: 22 June 2016  
© The Author(s) 2016. This article is published with open access at Springerlink.com

**Abstract** I perform a combined analysis of the ATLAS and CMS diphoton data, using both Run-I and Run-II results, including those released at the 2016 Moriond conference. I find combining the ATLAS and CMS results from Run-II increases the statistical significance of the reported 750 GeV anomaly, assuming a spin-0 mediator coupling to gluons or heavy quarks with a width much smaller than the detector resolution. This significance does not decrease when the 8 TeV data is included. A spin-2 mediator is disfavored compared to the spin-0 case. The cross section required to fit the ATLAS anomaly is in tension with the aggregate data, all of which prefers a smaller value. The best fit for all models I consider is a  $4.0\sigma$  local significance for a 750 GeV spin-0 mediator coupling to gluons with a cross section of 4 fb at 13 TeV (assuming narrow width) or 10 fb (assuming  $\Gamma = 45$  GeV).

## 1 Introduction

The ATLAS announcement [1] of a  $3.6\sigma$  local excess in diphotons with invariant masses near  $m_{\gamma\gamma} \sim 750$  GeV in the first batch of LHC Run-II data, combined with the CMS Collaboration announcing [2] a  $2.6\sigma$  local excess in the same channel and invariant mass, has sent the theoretical physics community into a frenzy of model-building, with 150 papers on the topic appearing on arXiv within a month. The “ $\gamma\gamma$  Resonance that Stole Christmas” [3] is of course tremendously exciting. It is the LHC’s most statistically significant deviation from the Standard Model of particle physics made public since the discovery of the 125 GeV Higgs boson. The addition of  $0.6 \text{ fb}^{-1}$  of CMS data gathered without the presence of the solenoid field [4], as well as a reanalysis of the 13 and 8 TeV data by the ATLAS Collaboration [5] has increased the statistical preference for new physics, with CMS now reporting a  $3.4\sigma$  local significance in their combined data.

At this stage, the information on which theorists can build models is somewhat minimal, assuming that these results are not just a somewhat unlikely statistical fluctuation and there is actually new physics to be begun with. A  $3.6\sigma$  signal is not very large, and additional slicing of the data in order to ask more detailed questions will typically yield only small statistical preference for any possible result. The goal of this paper is to investigate what information can be extracted from the combination of ATLAS and CMS data in the diphoton channel, including the most recent analyses released at the 2016 Moriond conference [4,5]. In particular, I am interested in the statistical significance of the combined 13 TeV Run-II data, and in the significance of combinations with the Run-I 8 TeV data. In addition, the ATLAS Collaboration claims a better fit ( $3.9\sigma$  local) to a resonance at 750 GeV with a width of 45 GeV, as opposed to a narrow resonance with width much less than the experimental resolution (as might be naively expected). Fitting this wide resonance into theoretical models has been the focus of many of the 150 papers on the topic. In this paper, I consider the combined statistical preference for this width.

This paper should be viewed as a follow-up to the work of Refs. [6–8], which are some of the earliest theoretical papers on the 750 GeV anomaly, and have largely set the parameters which later papers have adopted. Where our results overlap, my results broadly agree with those found in Refs. [6–8]; in particular in terms of the best-fit cross sections for the anomaly. This paper goes into somewhat more detail in fitting the signal in the ATLAS and CMS data, by floating the fit to the background functional forms as signal is added. I also perform fits to spin-2 resonances, and I investigate the preference of the combined data for a wide or narrow resonance. This paper does not attempt to address the implications of this anomaly for other search channels at the LHC, new physics models beyond the resonance itself, or a derivation of any limits on fundamental couplings. Such questions have been well addressed in the literature. I restrict this paper solely to the

<sup>a</sup>e-mail: mbuckley@physics.rutgers.edu

input parameters for theoretical studies: the cross sections, widths, and statistical significance of the anomaly itself.

The next section describes my combination fits to the ATLAS and CMS diphoton data, using both 13 and 8 TeV data. For simplicity (and due to the computational limitations of the event generation), I consider only local significance in my combination fits, rather than including the look-elsewhere-effect. The statistical question at hand here is the significance of the anomaly at 750 GeV specifically, thus somewhat justifying this choice. I parameterize the possible couplings of the mediator to gluons and light quarks separately, and consider both spin-0 and spin-2 resonances. I present additional results for second generation and  $b$ -quark couplings in Appendix A. In Sect. 3, I then turn to the question of the statistical preference for a wide or narrow resonance; using the best-fit parameters from Sect. 2. I will discuss my conclusions in Sect. 4, but I summarize some of the more salient points here:

1. The required cross section to fit the anomaly reported by ATLAS is in tension with the 8 TeV results, as well as the required cross section to fit the CMS anomaly.
2. Combining all data sets yields a local significance of  $\sim 4.0\sigma$  for a 750 GeV spin-0 resonance produced through couplings to gluons or heavy quarks. While quoted statistical significances must be taken with a grain of salt, as they are obtained using binned data without inclusion of systematic errors, I find the combination yields a net *increase* in the statistical significance as compared to the ATLAS data alone.
3. The spin-2 interpretation is mildly disfavored compared to a spin-0 mediator. This is due to correlations in the photon momenta which results in a relative decrease in the ATLAS acceptance compared to CMS.
4. The combination of ATLAS and CMS 13 TeV data has a slight statistical preference for a spin-0 mediator with a natural width much smaller than the experimental resolution, as compared to the  $\Gamma = 45$  GeV preferred by ATLAS alone. When the 8 TeV data is added, there is a slight statistical preference for a wide resonance over the narrow option, as it is easier to hide a wide resonance in the 8 TeV background.

## 2 Combination fits

In this section, I consider the ATLAS and CMS searches for diphoton resonances. There are six data sets to consider: the ATLAS [1] and CMS [2] Run-II searches at 13 TeV—which contain the anomalous excess that have caused so much excitement of late—and the previous 8 TeV Run-I diphoton resonance searches from the two experiments [9, 10]. CMS has a smaller data set, gathered when their solenoid magnetic

field was off during the 13 TeV Run-II [4], released at the Moriond 2016 conference. Note that ATLAS had two possible Run-I diphoton searches at the time of the announcement of the Run-II anomaly: one from the Higgs working group [9], and one from the exotica working group [11]. These have slightly different event selection criteria; the exotica search was developed to target spin-2 graviton searches, while the former is designed to search for Higgs-like scalar resonances. After the reanalysis of both Run-I and Run-II data released by ATLAS at the Moriond conference, a choice of two event selection criteria was applied to both the ATLAS 13 and the 8 TeV data sets, one targeted for spin-0 resonances, and the other for spin-2 [5]. In this paper, I use the appropriate ATLAS event selection as I consider the two spin options. For the remainder of this paper, I will refer to these six data sets by the names ATLAS13 [1, 5], CMS13 [2], CMS13/0T [4] (for the data collected when the magnetic field was 0 T), ATLAS8 [5], and CMS8 [10].

The selection criteria for each of the data sets vary slightly. In Table 1, I list the requirements for diphoton events to end up in the analysis region for each experimental search. In addition, each search implements isolation criteria on the photon candidates. CMS13 has two search regions, one where both photons are central (denoted “BB” here, for “barrel–barrel” events), and one where one photon is forward (“BE,” for barrel–endcap). The CMS13/0T data uses identical selection criteria. The CMS Collaboration analysis of their CMS8 results uses four signal regions, depending on whether the leading- and subleading- $p_T$  photons have converted in the detector. For the range of photon  $p_T$  of interest here, this level of distinction is less important, and for simplicity I used the combined CMS8 data set. Both the ATLAS13 and the ATLAS8 data use separate selection criteria for their spin-0 and spin-2 searches.

As a resonance search, we are interested in peak-like structures in the differential distribution of the diphoton invariant mass  $m_{\gamma\gamma}$ . As a first step, I verified my ability to reproduce the reported fits to the background functional forms, assuming no signal injected. In each analysis, the backgrounds are fit to a data-driven two-parameter function, assuming Poisson statistics. These functions are

$$\text{ATLAS8(ATLAS13)} : f(m_{\gamma\gamma}; a_0, b) = \left(1 - \left(\frac{m_{\gamma\gamma}}{\sqrt{s}}\right)^{1/3}\right)^b \left(\frac{m_{\gamma\gamma}}{\sqrt{s}}\right)^{a_0}, \quad (1)$$

$$\text{CMS13(CMS13/0T)} : f(m_{\gamma\gamma}; a, b) = m_{\gamma\gamma}^{a+b} \log m_{\gamma\gamma}, \quad (2)$$

$$\text{CMS8} : f(m_{\gamma\gamma}; p_1, p_2) = e^{-p_1 m_{\gamma\gamma}} m_{\gamma\gamma}^{-p_2}. \quad (3)$$

After digitizing the binned  $m_{\gamma\gamma}$  data from each experiment, I fit to these functional forms, marginalizing over the two free parameters assuming Poisson statistics. While the experiments themselves obviously have access to much more infor-

**Table 1** Selection criteria for the six experimental searches I consider in this paper. For CMS13 and CMS13/0T, events are divided into barrel-barrel (BB) and barrel-endcap (BE) categories. The column labeled “<  $|\eta|$  <” indicates the transition’s  $\eta$  region excluded from the selected

events. The dual upper limits on  $|\eta|$  for the CMS8-BE category indicate that one photon must be in the barrel ( $|\eta| < 1.44$ ) and one must be in the endcap ( $|\eta| < 2.5$ ). Two different selection criteria are used by ATLAS for their spin-0 and spin-2 analyses

	$\mathcal{L}$ (fb <sup>-1</sup> )	$E_{T1}$ (GeV)	$E_{T2}$ (GeV)	$ \eta  <$	$<  \eta  <$	$E_{T1}/m_{\gamma\gamma}$	$E_{T2}/m_{\gamma\gamma}$
ATLAS13 spin-0	3.2	40	30	2.47	1.37–1.52	0.4	0.3
ATLAS13 spin-2	3.2	55	55	2.47	1.37–1.52	–	–
CMS13(CMS13/0T)-BB	2.7(0.6)	75	75	1.44	–	–	–
CMS13(CMS13/0T)-BE	2.7(0.6)	75	75	1.44/2.5	1.44–1.57	–	–
ATLAS8 spin-0	20.3	22	22	2.37	1.37–1.56	0.4	0.3
ATLAS8 spin-2	20.3	50	50	2.37	1.37–1.56	–	–
CMS8	19.7	33	25	2.5	1.44–1.57	0.33	0.25

mation of the unbinned diphoton events, I am restricted to the public data, which is of course binned. This loss of information will result in some degradation of statistical power, as will be seen, but the difference is not large. My resulting best-fit backgrounds are shown in Fig. 1 (using the spin-0 selection for the ATLAS data) overlaid with the experimental data for the six experimental searches. In all cases, I can successfully reproduce the best-fit backgrounds found by the experimental collaborations.

It should be noted that these functional forms are data-driven, and out of six diphoton analyses, three different functional forms were chosen. It has been noted that changing the functional forms to increase support at high invariant mass could possibly reduce the significance of the observed excess [12]. This is made possible by the low statistics of diphoton counts at large  $m_{\gamma\gamma}$ . Further, the 750 GeV diphoton excess sits near the tail of the 8 TeV ATLAS and CMS analyses. Thus, it is possible to “hide” the 13 TeV excess in the 8 TeV by lowering the background function in this region and absorbing the excess into the signal. This is especially notable when the signal is assumed to be a wide resonance, covering much of the high  $m_{\gamma\gamma}$  range.

After fitting the background functions to the digitized data, I then use these background-only fits to validate my simulation pipeline. I simulate the primary irreducible background of  $pp \rightarrow \gamma\gamma + X$  using MADGRAPH5 [13], matched up to two jets at  $p_T = 10$  GeV using PYTHIA6 [14]. Detector simulation is performed using DELPHES3 [15], with the default ATLAS and CMS detector cards. A  $K$ -factor of between 1.4 and 1.8 was needed to match the experimental yields. The resulting distributions, normalized using the  $K$ -factors, are also shown in Fig. 1. While the simulated  $m_{\gamma\gamma}$  distribution is largely in good agreement, some deviation is observed at low invariant masses. This deviation is due to the lack of box diagrams in the MADGRAPH5 simulation. Fortunately this occurs far from the signal region. Therefore, this simulation technique should be acceptable for the generation of signal events.

I now turn to the excess at 750 GeV in the 13 TeV data. I fit the data to two possibilities: either a spin-0 or spin-2 particle decaying to two photons with a mass near 750 GeV.<sup>1</sup> In particular, I will discuss the agreement of the four data sets, and the preference in the data (if any) for a wide or narrow resonance.

### 2.1 Spin-0 resonance

Of the avalanche of theory papers discussing the ATLAS13 and CMS13 diphoton anomaly, the majority have considered the spin-0 scenario. Here, I take a model-independent approach, though I do specialize to the CP-even scalar option. The CP-odd pseudoscalar is also possible (see e.g. Ref. [17]), but will result in a very similar analysis. Using FEYN-RULES2.3 [18], I constructed MADGRAPH5 model files for a new scalar spin-0 particle with couplings to one of the following sets of partons:

1. Gluons (presumably mediated through a loop) via the interaction

$$\mathcal{L}_{\Phi-g} \supseteq c_g \Phi_g G^{\mu\nu,a} G_{\mu\nu}^a \tag{4}$$

2. Valance quark–antiquark ( $u/d$ ) pairs, through the interaction

$$\mathcal{L}_{\Phi-q} \supseteq c_q \Phi_q \left( \frac{m_u}{v} \bar{u}u + \frac{m_d}{v} \bar{d}d \right) \tag{5}$$

3. Charm and strange quark–antiquark pairs, through the interaction

$$\mathcal{L}_{\Phi-Q} \supseteq c_Q \Phi_Q \left( \frac{m_c}{v} \bar{c}c + \frac{m_s}{v} \bar{s}s \right) \tag{6}$$

<sup>1</sup> Spin-1 mediators decaying to diphotons are ruled out by the Landau–Yang theorem, though it may be possible to find gauge boson mediator solutions through sufficient theoretical model-building efforts [16].

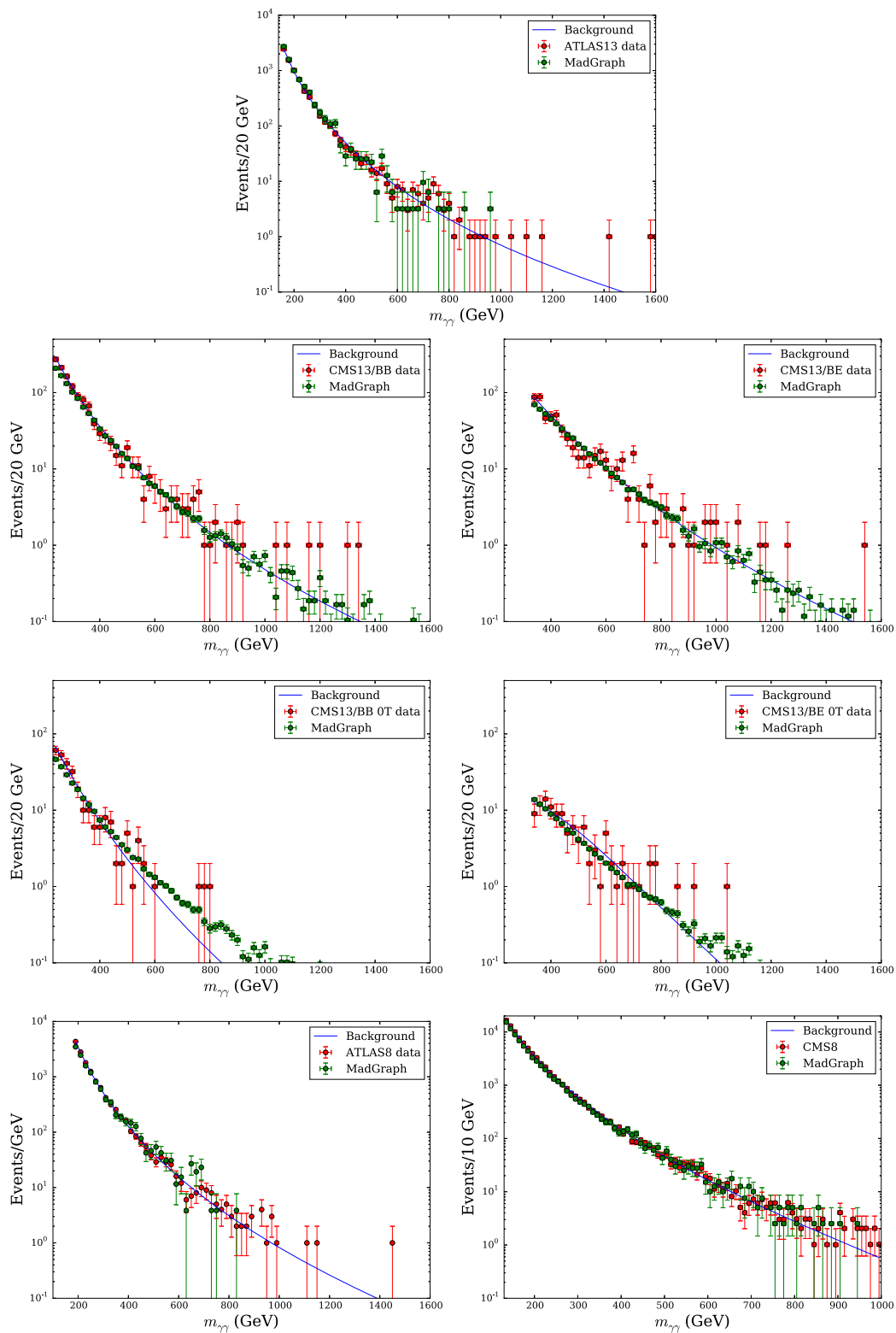


**Fig. 1** Digitized data (red points) from spin-0 ATLAS13 [1] (top), CMS13 [2] (CMS13/0T [4]) in the barrel–barrel (second (third) row left) and barrel–endcap (second (third)) categories, spin-0 ATLAS8 [9]

(lower left), and CMS8 [10] (lower right). Best-fit background functions Eqs. (1)–(3) are shown in blue. MADGRAPH5 simulated background events are shown in green

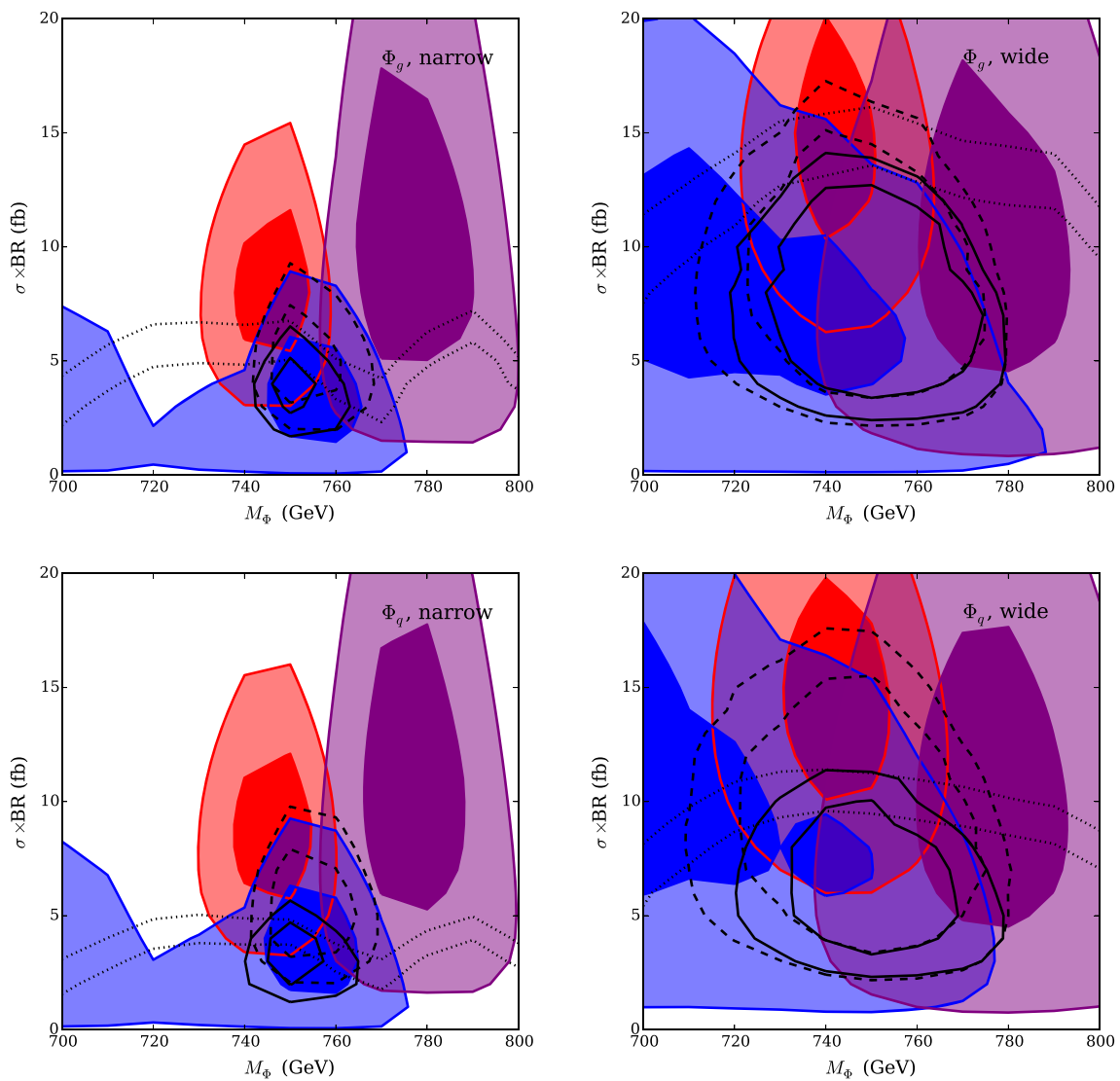


**Fig. 2** Best-fit regions (1 and  $2\sigma$ ) of a spin-0 mediator decaying to diphotons, as a function of mediator mass and 13 TeV cross section, assuming the indicated mediator couplings to partons and mediator width. Red regions are the 1 and  $2\sigma$  best-fit regions for the ATLAS13 data, blue is the fit to CMS13 data, and purple is the CMS13/0T. The combined best fit for both ATLAS13, CMS13, and CMS13/0T (COMBO13) are

4. Bottom quark–antiquark pairs, through

$$\mathcal{L}_{\Phi-b} \supseteq c_b \Phi_b \frac{m_b}{v} \bar{b}b. \tag{7}$$

Here  $v$  is the Standard Model Higgs vacuum expectation value  $v = 246$  GeV, and the  $c_i$  are couplings which can be floated to fit to the observed cross section. Assuming proportionality of interactions to the quark masses is motivated from Minimal Flavor Violation [19], but the following is not too sensitive to this assumption. In all cases, decays to photons are the result of the interaction

$$\mathcal{L}_{\Phi-\gamma} \supseteq c_\gamma \Phi F^{\mu\nu} F_{\mu\nu}. \tag{8}$$

the regions outlined in black dashed lines. The 1 and  $2\sigma$  upper limits from the combined 8 TeV data (COMBO8) are the black dashed lines (with cross sections converted to 13 TeV-equivalents). The best-fit signal combination of all six data sets (COMBO) are the black solid lines

The interactions are separated in this way to allow for more fine-grained investigation of the agreement of the 13 and 8 TeV data. If the anomaly is the result of a new particle at  $\sim 750$  GeV, the expected signal strength in each experiment should be related by the ratios of the relevant parton distribution functions (p.d.f.s). Any “realistic” theory for the anomaly could have couplings to more than one of these sets of partons; in such cases one can reweight the results of this paper. I also note that full, realistic simulation of the gluon coupling may require resolving the heavy colored particles running in the loop; this is relevant at values of the mediator  $p_T$  comparable to the mass of the particles in the loop [20]. Here I assume infinite masses, which presumably is a reason-



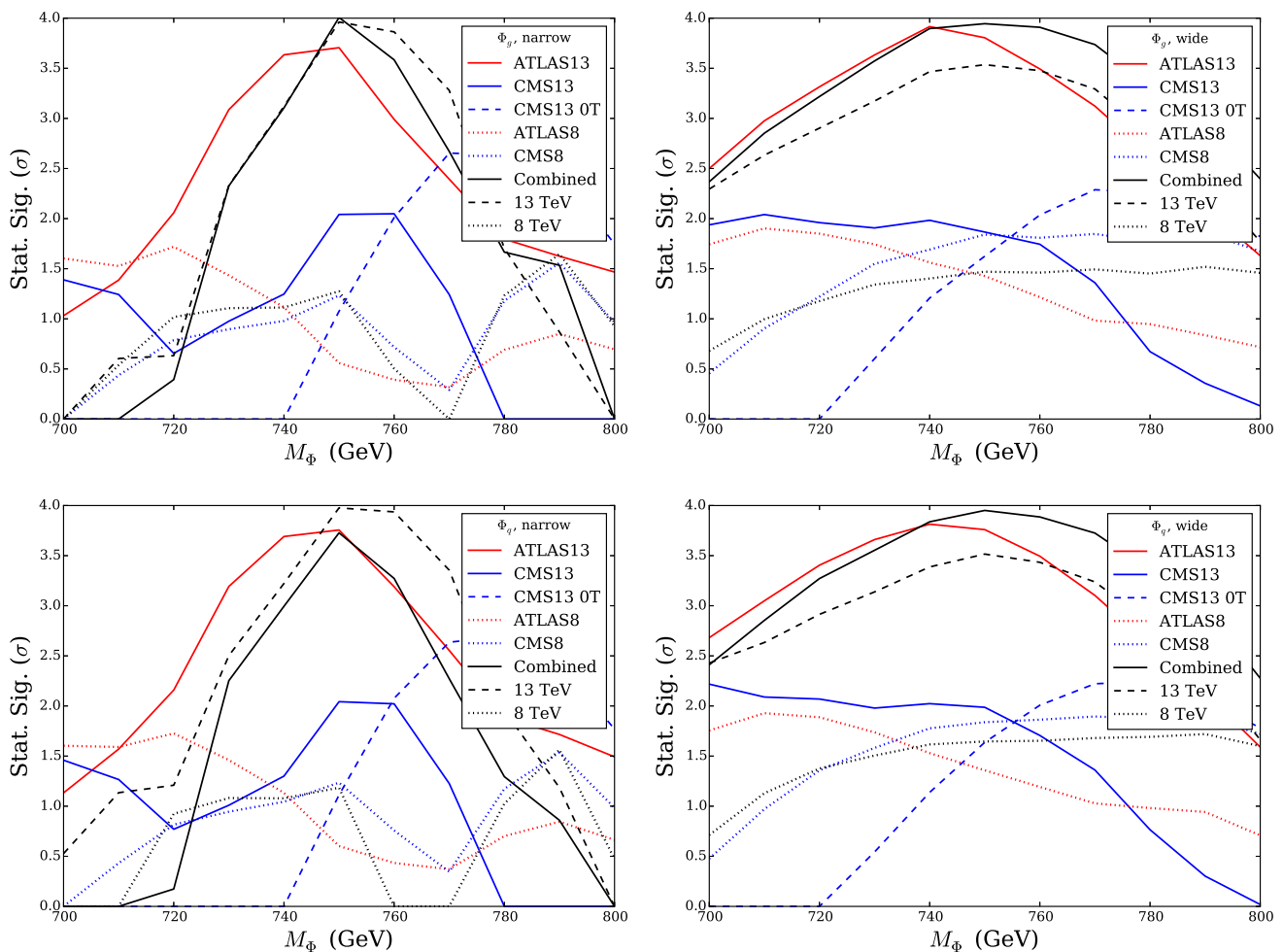


**Fig. 3** Statistical significance for a spin-0 mediator decaying to diphotons, as a function of mediator mass, assuming the indicated mediator couplings to partons and mediator width. At each mass, the cross section is set to the value that maximizes statistical significance for a signal (see Fig. 2). The solid red line is the statistical significance of the ATLAS13 data alone, solid blue is CMS13, dashed blue is CMS13/0T, and dotted

red and blue lines are ATLAS8 and CMS8, respectively. When comparing across experiments, note that these significances do not correspond to the same value of the cross section. The dashed (dotted) black line is the combination of 13(8) TeV data, requiring the same cross section in both ATLAS and CMS. The solid black line is the combined significance of all six data sets

able assumption for most models, as typically the mediator will be produced nearly at rest and the new colored mediators running the loop must be heavy. I also stress that my analysis assumes that the mediator producing the diphoton excess at  $m_{\gamma\gamma} \sim 750$  GeV is indeed a particle with mass near 750 GeV. It is possible that some heavier particle is produced, followed by a cascade decay resulting in the observed excess (see Ref. [6]). By increasing the mass of the mediator, the constraints from the 8 TeV data can be weakened, and only the direct comparison of ATLAS13 and CMS13 would be relevant.

For each model, I generated  $pp \rightarrow (\Phi \rightarrow \gamma\gamma) + X$  events, matched to two jets with a matching scale of 10 GeV, using the MADGRAPH5/PYTHIA6/DELPHES3 simulation chain described previously. No cuts were placed on the  $\Phi$  particles at the generator level. I scanned over mediator masses from 700 to 800 GeV, under two assumptions

of the width: narrow and wide. The narrow width mediator has a width set by the Lagrangian terms above (typically  $\Gamma \lesssim 50$  MeV), much less than the diphoton invariant mass resolution. The “wide” resonance has a width of  $\Gamma = 45$  GeV, as this is reported best-fit width in the ATLAS13 results. Scanning over the widths would be preferable to considering just these two assumptions. However, as I am considering only the binned data, the effective resolution of this scan is poor and extremely computationally intensive.

I find nearly flat signal acceptance for the range of mediator masses considered, for both the narrow and the wide hypotheses. The ATLAS13 analysis has an efficiency of  $\sim 50\%$  for spin-0 mediators—this is somewhat lower than the value quoted in Ref. [8]. The combined barrel–barrel and barrel–endcap CMS13 analysis has an efficiency of  $\sim 60\%$ , with 40% of events ending up in the barrel–barrel category, and 20% in the barrel–endcap. The CMS8 search also has a

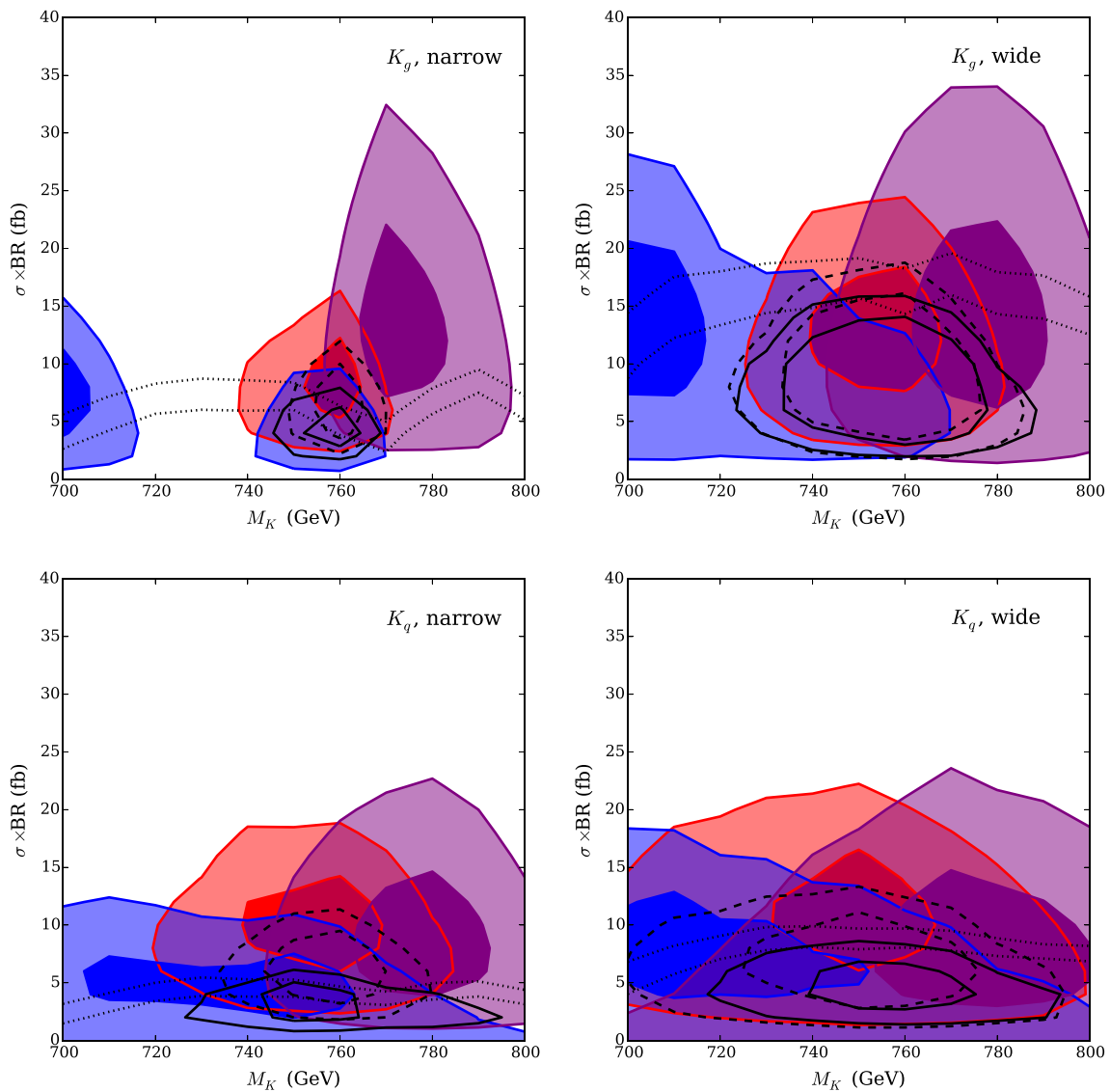


**Fig. 4** Best-fit regions (1 and  $2\sigma$ ) of a spin-2 mediator decaying to diphotons, as a function of mediator mass and 13 TeV cross section, assuming the indicated mediator couplings to partons and mediator width. *Red regions* are the 1 and  $2\sigma$  best-fit regions for the ATLAS13 data, *blue* is the fit to CMS13 data, and *purple* is the CMS13/0T. The combined best fit for both ATLAS13, CMS13, and CMS13/0T (COMBO13) are

the regions outlined in *black dashed lines*. The 1 and  $2\sigma$  upper limits from the combined 8 TeV data (COMBO8) are the *black dashed lines* (with cross sections converted to 13 TeV-equivalents). The best-fit signal combinations of all six data sets (COMBO) are the *black solid lines*

60% efficiency, while the ATLAS8 Higgs search is slightly less than this.

Using the  $m_{\gamma\gamma}$  distributions constructed from the simulated  $\Phi$  production and decay, I then fit the signal plus background to the data provided from each experiment, floating the normalization of the signal in terms of the production cross section times branching ratio into photons  $\sigma \times BR_{\gamma\gamma}$ . In each case, I refit the background distributions using the appropriate functional forms Eqs. (1)–(3), marginalizing over the background function parameters, and maximizing the log-likelihood assuming Poissonian statistics.

Production cross sections for the 8 TeV data are then reweighted to the 13 TeV results using MADGRAPH5 sim-

ulation to obtain the necessary p.d.f. factors. All cross sections quoted in this paper are in terms of the 13 TeV data, and they are thus directly comparable. The ratios of 13 TeV cross sections to 8 TeV cross sections (for both wide and narrow resonances) are nearly independent of resonance mass in the 700–800 GeV range considered here. For scalar mediators coupling to gluons ( $\Phi_g$ ), this ratio is  $\sim 4.5$ , for couplings to valence quarks ( $\Phi_q$ ) it is  $\sim 3.1$ , for couplings to  $s/c$  quarks ( $\Phi_Q$ ) it is  $\sim 4.2$ , and  $\sim 4.0$  for bottom quarks ( $\Phi_b$ ). These cross section ratios come from two-jet matching, and so include initial states other than those that couple directly to the mediator in question. Due to the similarity of the  $\Phi_g$ ,  $\Phi_b$ , and  $\Phi_Q$  p.d.f. ratios, I will show only

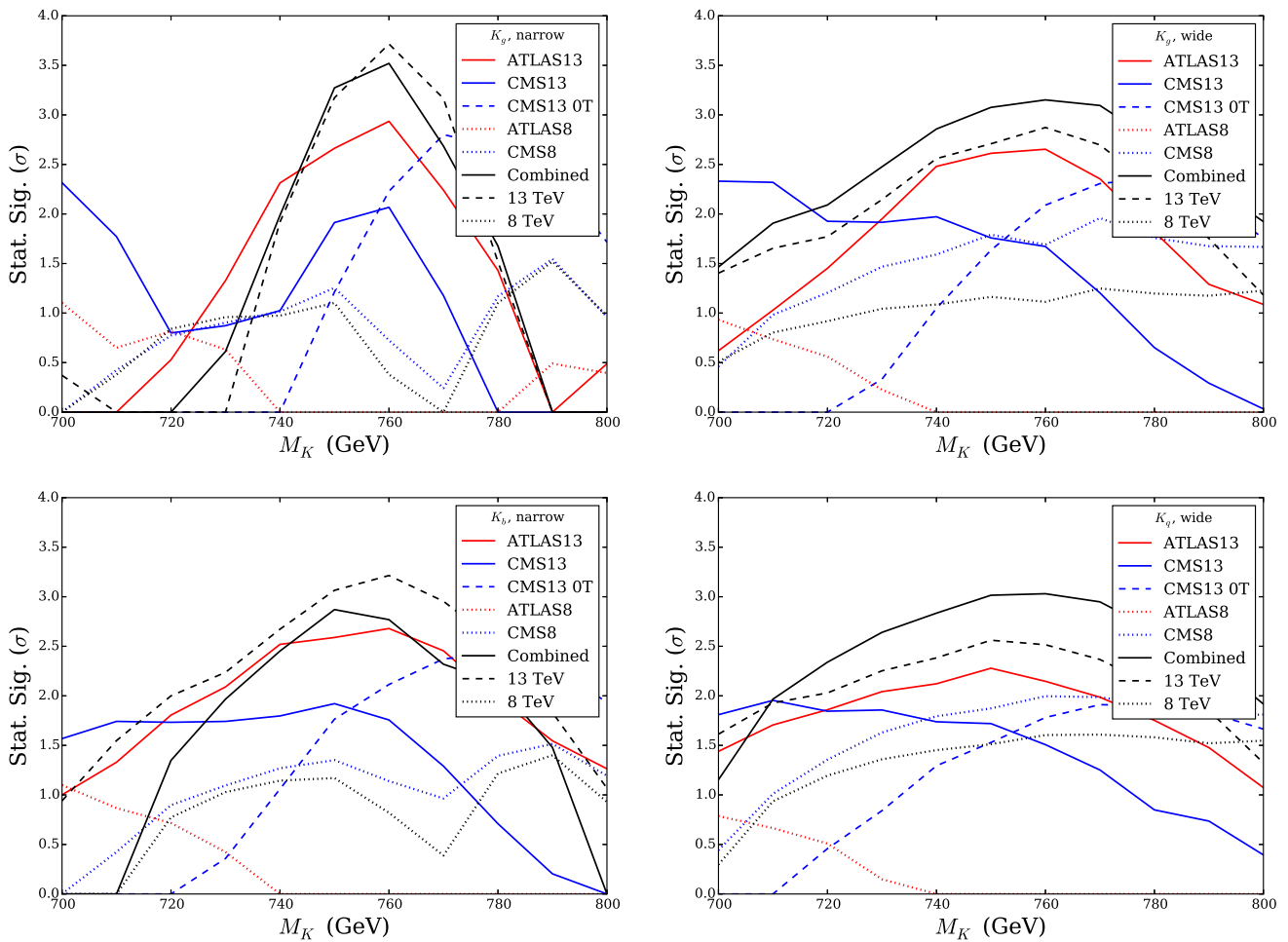


**Fig. 5** Statistical significance for a spin-2 mediator decaying to diphoton, as a function of mediator mass, assuming the indicated mediator couplings to partons and mediator width. At each mass, the cross section is set to the value that maximizes statistical significance for a signal (see Fig. 2). The *solid red line* is the statistical significance of the ATLAS13 data alone, *solid blue* is CMS13, *dashed blue* is CMS13/0T, and *dotted*

*red and blue lines* are ATLAS8 and CMS8, respectively. When comparing across experiments, note that these significances do not correspond to the same value of the cross section. The *dashed (dotted) black line* is the combination of 13(8) TeV data, requiring the same cross section in both ATLAS and CMS. The *solid black line* is the combined significance of all six data sets

$\Phi_g$  in this section and relegate the  $\Phi_b$  and  $\Phi_Q$  results to Appendix A.

Using the fitting procedure described, in Fig. 2, I show the best-fit values for the cross sections' time branching ratios into photons, as a function of resonance mass (again, for both choices of overall width). The statistical significance of these best-fit excesses are shown in Fig. 3 (for  $\Phi_Q$  and  $\Phi_b$  interpretations, see Figs. 8 and 9 in Appendix A). The statistical significance is obtained from the  $\Delta \log$  likelihood assuming a single degree of freedom. Best-fit  $\sigma \times \text{BR}$  and statistical significances are shown individually for the ATLAS13 and CMS13 data sets; as is by now well-understood, these analyses show an excess near 750 GeV. Adding in the CMS13/0T data also shows some preference for a signal slightly about 750 GeV.

My statistical fits must be compared with the quoted values from the ATLAS and CMS Collaborations themselves. For

ATLAS13, I find a local statistics-only significance for a narrow signal of  $\sim 3.6\sigma$  for a particle with a mass of 750 GeV. I further find a marginal improvement to the local significance (up to  $\sim 3.9\sigma$ ) for the  $\Gamma = 45$  GeV hypothesis. The full experimental analysis finds  $3.6\sigma$  for the narrow width and  $3.9\sigma$  for the wider resonance, using the unbinned data and including systematic errors which are not replicable in a theory analysis—though the exact agreement of my numbers with the experimental results must be seen as coincidental. For the CMS13 data, I find a local statistical significance of  $2.0\sigma$  for the narrow width hypothesis, while the CMS Collaboration found a local significance of  $2.6\sigma$ . Thus, my results combining the data sets are also likely to be underestimations of the true significance of various combinations of data sets (despite the fact that I have neglected systematic errors), though of course one cannot be sure barring a full experimental analysis.



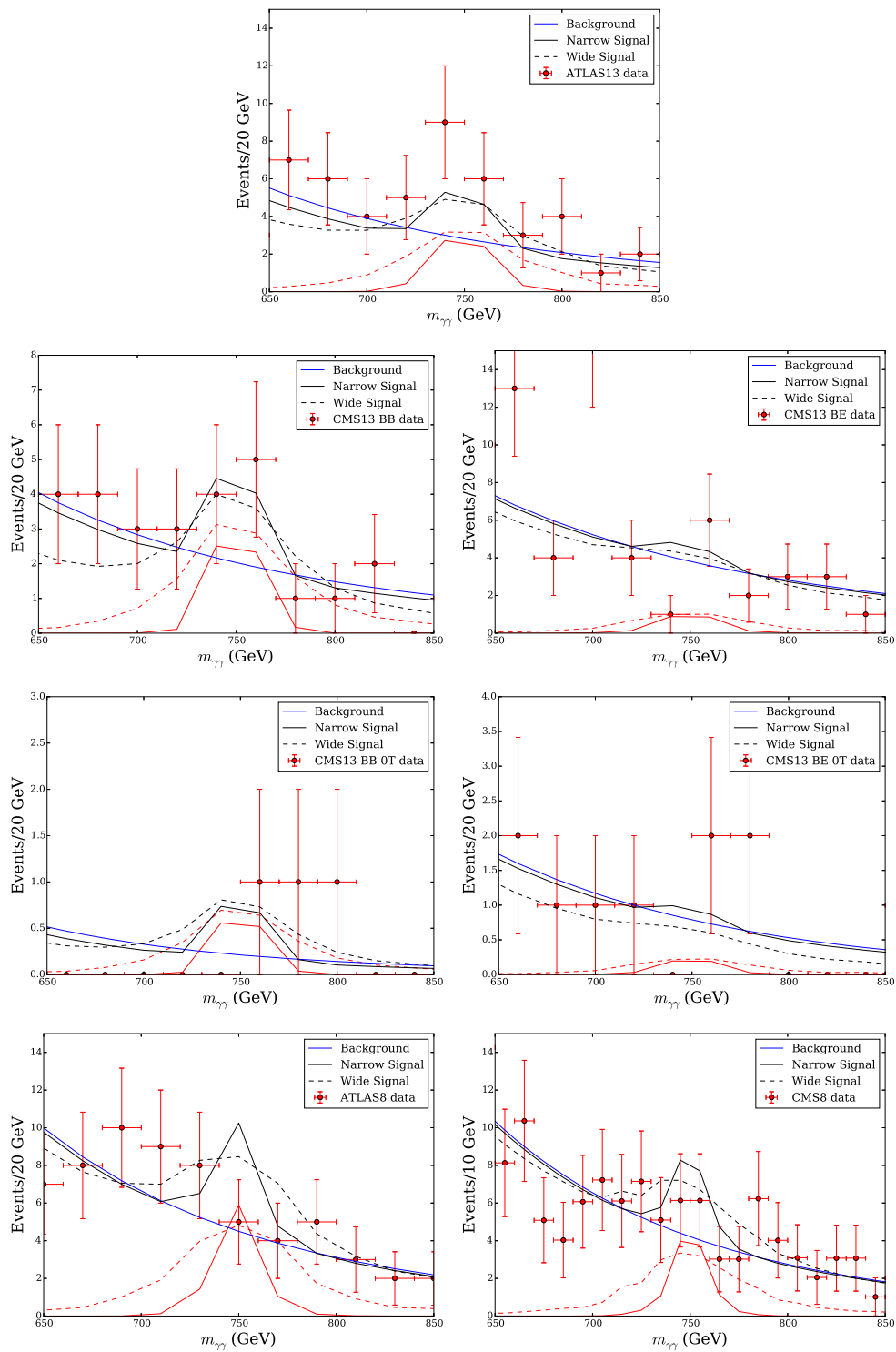


**Fig. 6** Zoomed-in data (red points) for ATLAS13 (top row), CMS13 (CMS13/OT) (barrel–barrel second (third) row left and barrel–endcap second (third) row right), ATLAS8 (lower left), and CMS8 (lower right). Also shown are the best-fit binned differential distributions for a 750 GeV scalar resonance, with a 13 TeV cross section of 4 fb (narrow,

solid red line), and 10 fb (wide, dashed red line). The best-fit background is shown in blue, and the sum of background and signal are the solid (dashed) black lines for the narrow (wide) signal. The background is refit to maximize the log-likelihood in the presence of the signal

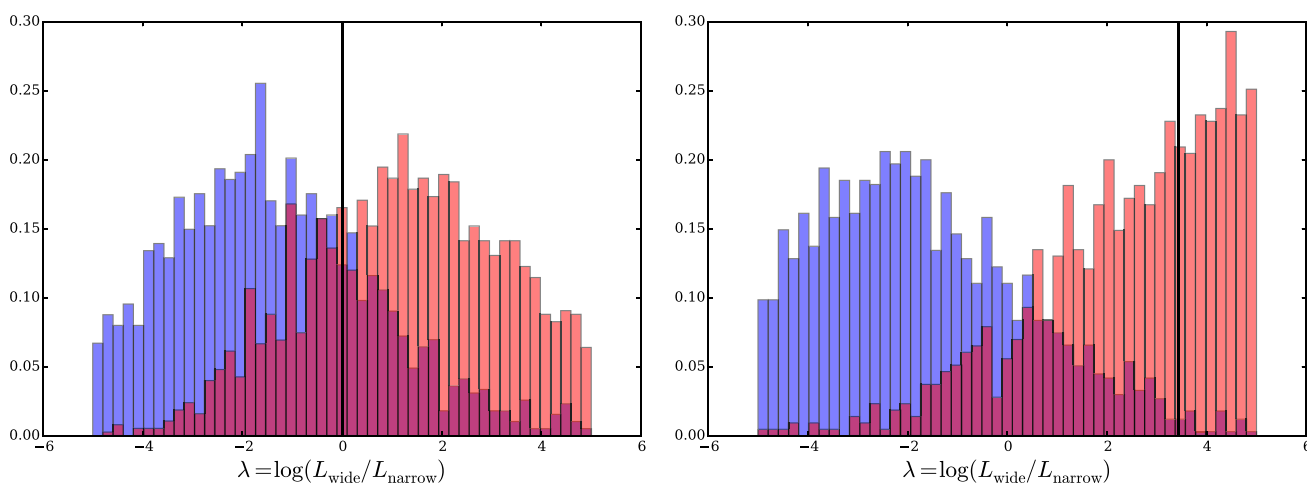


**Fig. 7** Histograms of  $\Delta \log$  likelihood of the COMBO13 (*left*) and COMBO (*right*) fit to the wide- and narrow-resonance interpretation of the diphoton anomaly. The *blue histograms* represent 2000 pseudoexperiments where a narrow 750 GeV signal was injected to the ATLAS and CMS data with a cross section of 4 fb and then fit to both a narrow

and wide template. The *red histogram* represent 2000 pseudoexperiments generated where a wide 750 GeV signal was injected with a cross section of 10 fb, then fit to both signal templates. The *black vertical line* is the value of  $\lambda = \log L_{\text{wide}}/L_{\text{narrow}}$  found in the real data ( $\lambda_o$ ), and the relative bin heights at  $\lambda_o$  give the likelihood ratio  $R$

Going further, I next consider the evidence for an excess in combinations of the data sets. Looking first at the 13 TeV data, I test the statistical significance of a single resonance with a common  $\sigma \times \text{BR}$  in the ATLAS13, CMS13, and CMS13/OT data. This “COMBO13” result prefers a signal at 750 GeV with a cross section between the ATLAS13 and CMS13 value, as expected. More interesting perhaps is the change in the statistical significance of this excess: for narrow widths, the COMBO13 best-fit cross section of  $\sim 5$  fb is preferred at  $\sim 3.9\sigma$ . This is an increase from the ATLAS13 individual fit, but below the naive expectation one might have from combining the ATLAS13, CMS13, and CMS13/OT significances ( $\sim \sqrt{(3.6\sigma)^2 + (2.0\sigma)^2 + (2.5\sigma)^2} = 4.8\sigma$ ), as the best-fit cross sections and masses for the three experimental analyses disagree. For wide resonances, combining the ATLAS13 and CMS13 data results in a net decrease in the statistical significance relative to the ATLAS13 data, to  $\sim 3.4\sigma$ . This is the first indication that the wide resonance seen by ATLAS is disfavored by the CMS results.

The preceding set of statements is largely independent of the type of the coupling between the mediator and the proton’s partons. However, when adding in the 8 TeV data, I must specify the coupling in order to determine the 8 TeV cross section which is equivalent to the 13 TeV value. For my purposes, it suffices to discuss the coupling to gluons and compare to the coupling to the valence  $u/d$  quarks, as couplings to other quark flavors have similar p.d.f.s to gluons and thus have very similar conclusions. As can be seen in Fig. 2, the combined 8 TeV data disfavors the ATLAS13 best-fit cross section for a narrow width at  $1\sigma$ .

However, if I instead ask for the best-fit region for a single cross section fitting both the 13 and the 8 TeV data, I

find that there is a good fit for a narrow resonance at a 4 fb cross section, close to the CMS13 value, assuming a gluon coupling. This is within the  $1\sigma$  region for CMS13, within  $2\sigma$  of ATLAS13, and is less than  $1\sigma$  tension with the 8 TeV data. The statistical preference for this signal is identical to the combined fit to ATLAS13 and CMS13, at about  $4.0\sigma$ .

In the wide-resonance interpretation, the 8 TeV data is much less constraining. While the combination of ATLAS13 and CMS13 data reduces the preference for a wide signal, adding the 8 TeV data returns the total statistical significance to  $\sim 4.0\sigma$  assuming couplings to gluons—about the same significance as ATLAS13 alone. This is driven by the ability for the background models of the 8 TeV data to absorb the signal without resulting in any large excess above the observed smooth distribution. The insensitivity of the 8 TeV data to the broad excess is enough to hide even that larger cross sections required by the light-quark coupling.

## 2.2 Spin-2 resonance

I now turn to the spin-2 possibility. My general approach is the same as in Sect. 2.1: I investigate individual couplings to the partons one-by-one, in order to make comparisons between the 8 and 13 TeV data. The mediator here is based on a spin-2 Kaluza–Klein graviton  $K$ , as implemented in MADGRAPH5 by Ref. [21] (see also Refs. [22–24]). I modified the relevant couplings to limit the interactions to gluons, light quarks, second-generation quarks, or bottom quarks. In all cases, the coupling to photons is generated through the simplified interaction

$$\mathcal{L}_{K-\gamma} \supseteq c_\gamma K^{\mu\nu} T_{\gamma,\mu\nu}, \quad (9)$$

$$T_\gamma^{\mu\nu} = \eta^{\mu\nu} \left( -\frac{1}{4} F^{\rho\sigma} F_{\rho\sigma} + (\partial_\rho \partial_\sigma A^\sigma) A^\rho + \frac{1}{2} \partial_\rho A^\rho \partial_\sigma A^\sigma \right) - F^{\mu\rho} F_\rho^\nu + (\partial^\mu \partial_\rho A^\rho) A^\nu + (\partial^\nu \partial_\rho A^\rho) A^\mu. \tag{10}$$

The terms involving  $A$  fields are gauge-fixing terms in the Feynman gauge. The stress-energy tensor for a quark  $q$ , relevant for the  $K$ -quarks interaction, is given by

$$T^{\mu\nu} = -i\eta^{\mu\nu} \left( \bar{q}\gamma^\rho \partial_\rho q - \frac{1}{2} \partial^\rho (\bar{q}\gamma_\rho q) \right) + \frac{i}{2} \left( \bar{q}\gamma^\mu \partial^\nu q + \bar{q}\gamma^\nu \partial^\mu q - \frac{1}{2} \partial^\mu (\bar{q}\gamma^\nu q) - \frac{1}{2} \partial^\nu (\bar{q}\gamma^\mu q) \right). \tag{11}$$

The production is through one of the following interactions:

1. Gluons, through the operator

$$\mathcal{L}_{K-g} \supseteq c_g K_g^{\mu\nu} T_{g,\mu\nu}, \tag{12}$$

$$T_g^{\mu\nu} = \eta^{\mu\nu} \left( -\frac{1}{4} G^{a,\rho\sigma} G_{\rho\sigma}^a + (\partial_\rho \partial_\sigma G^{a,\sigma}) G^{a,\rho} + \frac{1}{2} \partial_\rho G^{a,\rho} \partial_\sigma G^{a,\sigma} \right) - G^{a,\mu\rho} G_\rho^{a,\nu} + (\partial^\mu \partial_\rho G^{a,\rho}) G^{a,\nu} + (\partial^\nu \partial_\rho G^{a,\rho}) G^{a,\mu}. \tag{13}$$

2. Light valence quarks,  $u/d$ , through the interaction

$$\mathcal{L}_{K-q} \supseteq c_q K_q^{\mu\nu} T_{q,\mu\nu}, \tag{14}$$

where  $T_q^{\mu\nu}$  is the stress-energy tensor, Eq. (11) with  $q = u/d$ .

3. Second-generation quarks,  $s/c$ , through

$$\mathcal{L}_{K-Q} \supseteq c_Q K_Q^{\mu\nu} T_{Q,\mu\nu}, \tag{15}$$

where  $T_Q^{\mu\nu}$  is the stress-energy tensor, Eq. (11) with  $q = s/c$ .

4. The bottom quark, through

$$\mathcal{L}_{K-b} \supseteq c_b K_b^{\mu\nu} T_{b,\mu\nu}, \tag{16}$$

where  $T_b^{\mu\nu}$  is the stress-energy tensor, Eq. (11) with  $q = b$ .

The major difference in the analysis when compared to the spin-0 case is change in acceptance of the experiments to diphoton events. These changes are different for each of the six experimental searches I consider. After the ATLAS reanalysis from the 2016 Moriond conference, which uses

a separate set of selection criteria for the spin-0 and spin-2 searches, I find that spin-2 signal events have an acceptance of  $\sim 55\%$  in ATLAS13 and ATLAS8 for 750 GeV mediators. This is essentially the same as the acceptance for spin-0 mediators in these experiments. However, there are 75% more events in the spin-2 analysis. I find the barrel–barrel CMS13(CMS13/0T) signal acceptance is  $\sim 35\%$ , while the barrel–endcap signal acceptance is 25%, for a combined efficiency of nearly 60%, essentially the same as for the spin-0 case. The acceptance of spin-2 signals for CMS8 is 45%, a significant drop from the 60% acceptance for spin-0 signals.

In Fig. 4, I show the best-fit regions for signal cross section as a function of mediator mass for the  $K$  particle coupling to gluons or light quarks (couplings to  $c/s$  or  $b$  quarks are shown in Fig. 10, and they are very similar to those for gluons). The statistical significance of the best-fit cross sections are shown in Fig. 5. I find that the combined data sets disfavors the spin-2 mediator when compared to the spin-0, with a combined statistical significance of  $\sim 3.5\sigma$  for a narrow gluon-initiated resonance. This preference appears to be largely driven by the lower statistical preference for a spin-2 mediator in the ATLAS13 data. However, it must be stressed that the changes in statistical significance discussed here are less than  $1\sigma$ , and so are at best examples of mild preferences in the data.

### 3 Narrow or wide?

Now I attempt to address the question of whether there is any preference in the data for a wide resonance over a narrow one. For computational simplicity, I consider the best-fit scenario from Sect. 2: a scalar mediator coupling to gluons, with a cross section of 4 fb for the narrow resonance, and 10 fb for the broad resonance. As before, I do not scan over the width, but simply compare the narrow resonance (where the LHC width is controlled entirely by the detector resolution) with a mediator with a 45 GeV width, as suggested by the ATLAS13 results. In Fig. 6, I show the experimental data around the 750 GeV  $m_{\gamma\gamma}$  bins, compared to the predicted differential distributions of these best-fit points. It is clear from these examples why the wide resonance is in more tension with the CMS13 result, as well as why the 8 TeV data can more easily absorb this type of signal.

I have already discussed some of the statistical evidence for the question of narrow or wide resonances in the previous section. The combination of ATLAS13, CMS13, CMS13/0T increases the overall significance for a narrow resonance, and this significance does not decrease when the 8 TeV data is added, while the combination of 13 TeV data decreases the significance for a wide resonance (though this then increases once the 8 TeV data is included). Thus, one can say that both interpretations have equal statistical significance when combining all the data, though it is true that the combination of the 13 TeV alone mildly prefers the narrow resonance.

I perform one additional statistical test, calculating the likelihood ratio for the preference for the narrow resonance over a wide resonance. This is the ratio of the probability of observing some set of data given a narrow resonance over the probability of observing that data given the wide resonance. To calculate this, I define the log-likelihood ratio

$$\lambda = \log(L_{\text{wide}}/L_{\text{narrow}}), \quad (17)$$

where the  $L$  values are the maximum likelihoods (given an assumption of the width) marginalized over the background fit parameters. After calculating the *observed*  $\lambda_o$  from the data, I estimate the probability distribution by generating pseudoexperiments: injecting either a narrow or wide signal (with the best-fit cross section) over the best-fit background, and then calculating the  $\lambda$  value of that particular pseudoexperiment. The likelihood ratio  $R$  is then the ratio at  $\lambda_o$  of the normalized probability distribution for narrow signal over the distribution for a wide signal. In Fig. 7, I show these probability distributions along with the  $\lambda_o$  fit to the combination of ATLAS13 and CMS13 (left panel), and fit to all data (right panel). As can be seen, when considering only 13 TeV data, there is a very slight preference for a narrow resonance, with a corresponding ratio of  $R \sim 1$ , which indicates no significance preference for either model using the 13 TeV data only.

When combining all data, the likelihood ratio for the wide resonance over the narrow width is  $R \sim 20$ . Thus, if one is considering only the Run-II data, there is no particular preference for a wide or narrow width using this test, while if all data is considered, the 45 GeV width is somewhat more probable. However, it certainly should not be stated that we *know* with any degree of confidence that the proposed 750 GeV resonance has a width much larger than one might expect from a perturbatively coupled spin-0 mediator.

#### 4 Conclusions

When considering the 750 GeV diphoton excess, the theoretical community must balance its natural exuberance with the recognition that the statistical size of the anomalies are very small. As a result, any further slicing of data will yield at best modest statistical preferences for the phenomenological questions that we in the community want answers to. That said, given that this excess is the most significant seen at the LHC since the discovery of the 125 GeV Higgs, and the resulting avalanche of theoretical papers which shows no sign of slowing, it is still a useful exercise to carefully analyze the available data and determine what we do – and do not – know at this stage. While there is some useful information to be gleaned from this exercise, we are fortunate that the continuation of Run-II will be upon us shortly.

From the existing data, we can conclude the following:

1. Explaining the anomaly through a spin-0 resonance is preferred over a spin-2 mediator, though this preference is less than  $1\sigma$  in most cases.
2. Combining the 8 and 13 TeV data from ATLAS and CMS sets yields a  $\sim 4.0\sigma$  statistical preference for a signal of  $\sim 4(10)$  fb, assuming a narrow (wide) spin-0 resonance. This ignores the look-elsewhere effect, as discussed. Given that the significance of my fits to individual ATLAS and CMS data sets are underestimates when compared to the full experimental results, it is possible that the actual statistical preferences are larger than these quoted values. However, this would require a combined analysis performed by the ATLAS and CMS Collaborations.
3. The cross sections needed for the ATLAS13, CMS13, and CMS13/0T data sets are incompatible at the two sigma level, though they agree in mass. The most straightforward reading of this (while maintaining a new physics explanation for the anomalies) is that the larger ATLAS13 cross section constitutes a modest upward fluctuation from the “true” cross section, which is more in line with the CMS13 value.<sup>2</sup> The reverse is also possible of course, but it would bring the diphoton excess in the 13 TeV data in greater tension with the 8 TeV null results.
4. When considering only the 13 TeV data, the CMS13 data does not share the ATLAS13 preference for a 45 GeV width. I find that the “wide” interpretation of the resonance has a statistical significance in the COMBO13 data set which is approximately  $0.5\sigma$  less likely than the “narrow” interpretation. The corresponding likelihood ratio shows no preference for either width. Thus, while the theoretical challenge of a wide resonance may be appealing, the data in no way *requires* any new physics explanation to have the unusually large width of  $\Gamma \sim 45$  GeV.
5. Combining the 13 TeV data with the 8 TeV, I find that gluon-initiated mediators are preferred, due to having the largest ratio of relevant p.d.f.s. In particular, the combination of all six data sets for a gluon-initiated narrow resonance has the same statistical preference for a signal as the COMBO13 data alone does, though the best-fit cross section decreases slightly when the 8 TeV data is added ( $\sim 4.0\sigma$  for a  $\sim 4$  fb signal). In the narrow width assumption, heavy-quark-initiated mediators have slightly smaller statistical preference, and a light-quark coupling has a fairly significant decrease in statistical preference, indicating a more serious conflict between the 13 and 8 TeV data.

<sup>2</sup> Of course, in this interpretation, had the ATLAS13 data not had an upward fluctuation the combined statistical significance would likely not have been large enough to generate the massive response from the theoretical community. Thus, one may be tempted to take an anthropic principle view: an upward fluctuation in at least one of the data sets was a necessary condition for this paper to exist.

6. Combining the 13 and 8 TeV data sets under the  $\Gamma = 45$  GeV spin-0 model increases the statistical preference for signal as compared to the COMBO13 result, as the excess can be more easily absorbed by the background model here. Combining all the data sets in this way results in a  $\sim 3.5\sigma$  preference for a  $\sim 10$  fb signal (a  $0.5\sigma$  increase over the COMBO13 wide-resonance fit), with a likelihood ratio of  $\sim 20$  rejecting the narrow interpretation. Again, these statistical preferences are relatively small, thus theorists are free to explore the options, but should keep in mind that the experimental results are inconclusive.

The conclusions of this paper are perhaps not a surprise. There is a clear tension between the ATLAS13 and CMS13 results, as well as with the non-observation in 8 TeV data. The question of the width is especially puzzling; but further slicing of the data, as I have demonstrated, leads to somewhat conflicting results which do not have a clear statistical preference toward any particular solution. I note that if the ATLAS excess is indeed an upward fluctuation from a signal which is more in line with the CMS13 value, then perhaps this could also give a spurious signal of large width. However, the true answers will only come with more data, though I note that, if the signal is indeed real, but on the order of 4 fb, then we may need  $10\text{--}20\text{ fb}^{-1}$  for a single experiment to have  $5\sigma$  discovery.

**Acknowledgments** I thank Matthew Baumgart, JP Chou, Yuri Gershtein, Marco Farina, Angelo Monteux, David Shih, and Scott Thomas for useful feedback and discussions while writing this paper.

**Open Access** This article is distributed under the terms of the Creative Commons Attribution 4.0 International License (<http://creativecommons.org/licenses/by/4.0/>), which permits unrestricted use, distribution, and reproduction in any medium, provided you give appropriate credit to the original author(s) and the source, provide a link to the Creative Commons license, and indicate if changes were made. Funded by SCOAP<sup>3</sup>.

## Appendix A: Additional analysis

In the main body of the paper, I presented the best-fit cross sections and statistical significances of spin-0 and spin-2 mediators coupling to gluons and light  $u/d$  quarks. Couplings to  $c/s$  and  $b$  quarks in the proton are also possible, and here I present the equivalent results. As the ratio of p.d.f.s for these partons between 8 and 13 TeV is very close to that found for gluons, these results match the gluon plots in most respects. Figures 8 and 9 show the spin-0 best-fit cross sections and statistical significances for  $c/s$  and  $b$  couplings, while the spin-2 cases are shown in Figs. 10 and 11.

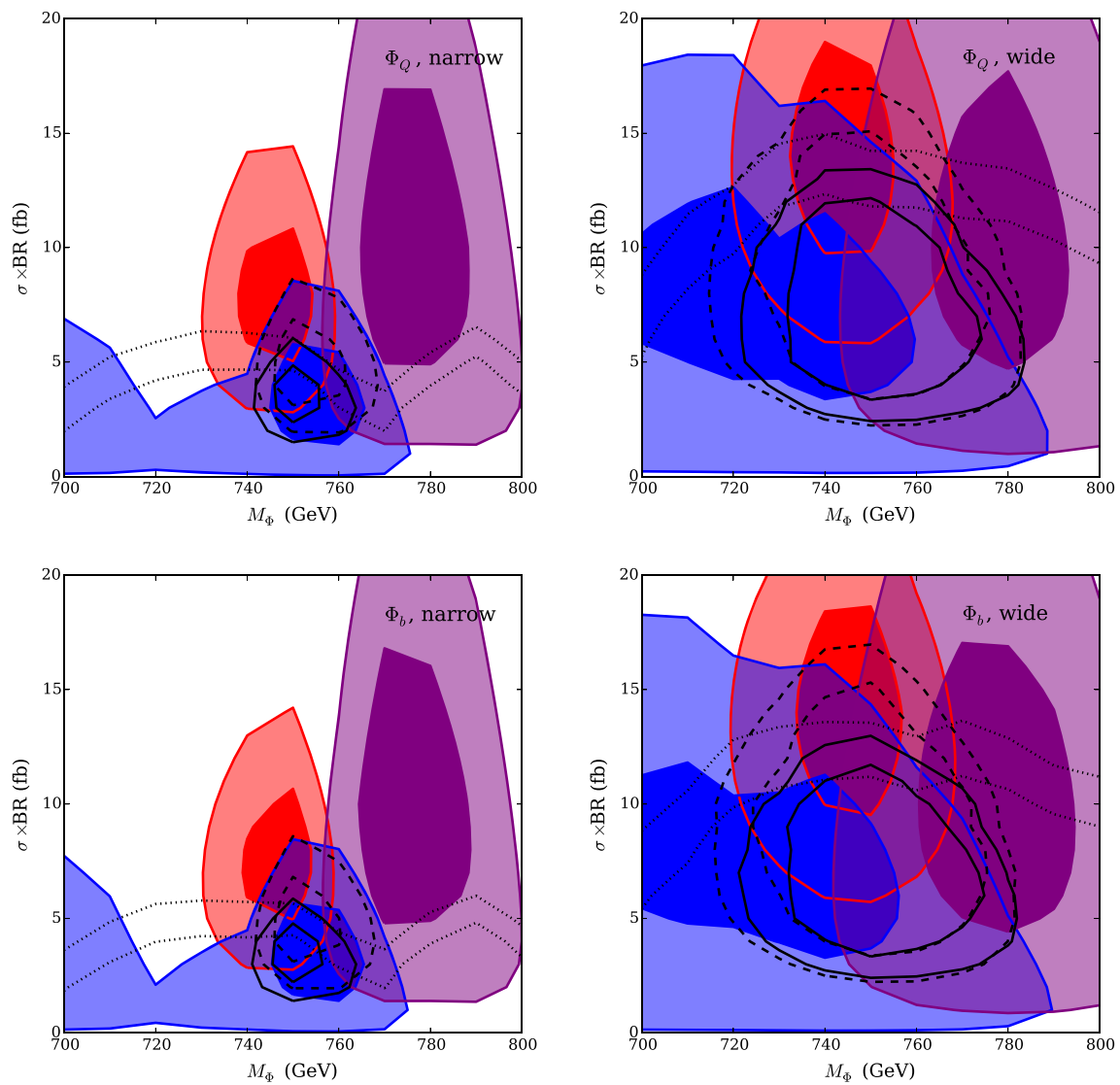


**Fig. 8** Best-fit regions ( $1$  and  $2\sigma$ ) of a spin-0 mediator decaying to diphotons, as a function of mediator mass and 13 TeV cross section, assuming the indicated mediator couplings to partons and mediator width. *Red regions* are the  $1$  and  $2\sigma$  best-fit regions for the ATLAS13 data, blue is the fit to CMS13 data. The combined best fit for both

ATLAS13 and CMS13 (COMBO13) are the regions outlined in *black dashed lines*. The  $1$  and  $2\sigma$  upper limits from the combined 8 TeV data (COMBO8) are the *black dashed regions* (with cross sections converted to 13 TeV-equivalents). The best-fit signal combination of all four data sets (COMBO) is the *black solid regions*



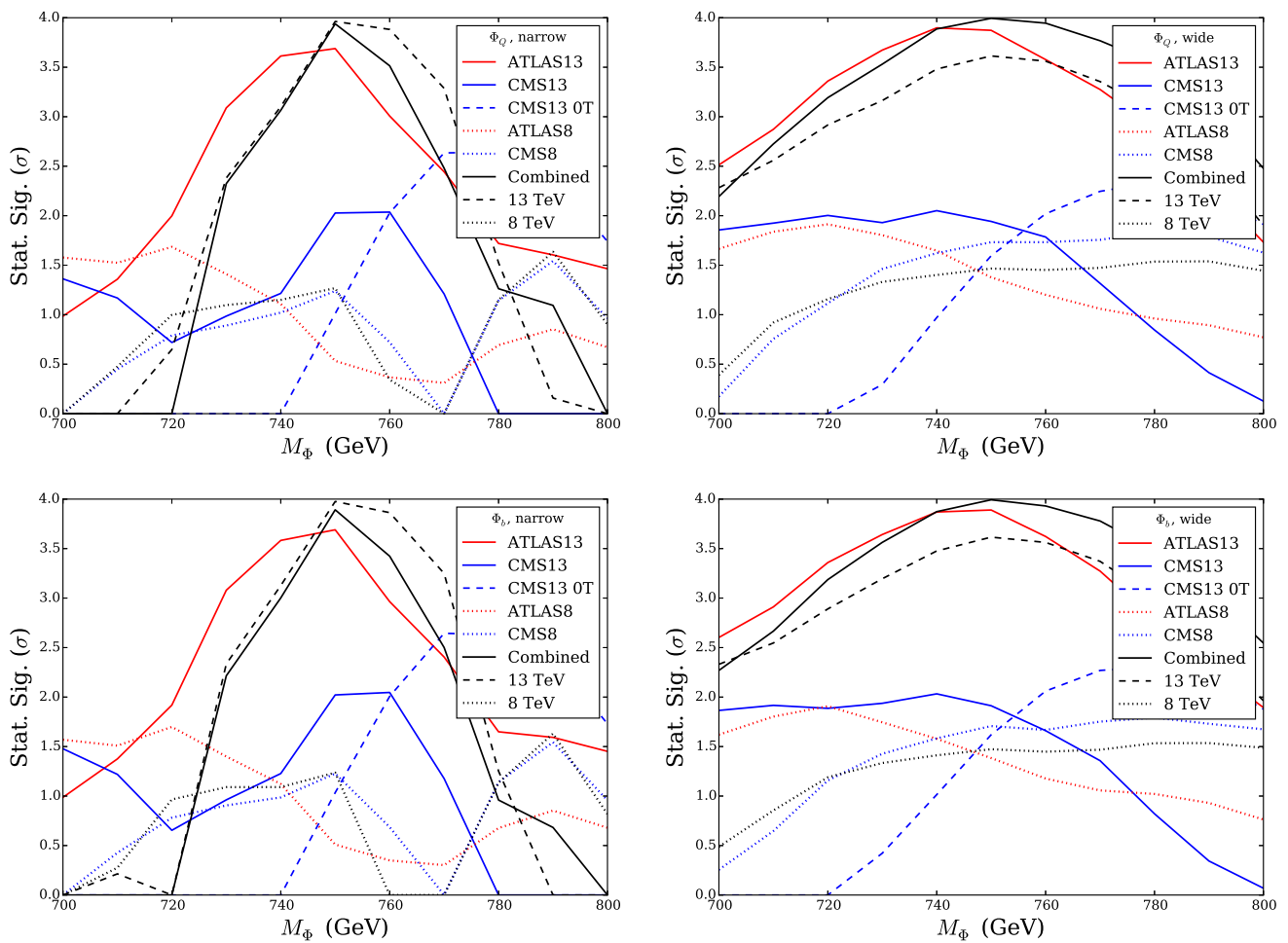


**Fig. 9** Statistical significance for a spin-0 mediator decaying to diphoton, as a function of mediator mass, assuming the indicated mediator couplings to partons and mediator width. At each mass, the cross section is set to the value that maximizes statistical significance for a signal (see Fig. 2). The *solid red line* is the statistical significance of the ATLAS13 data alone, *solid blue* is CMS13, and *dotted red and blue lines*

are ATLAS8 and CMS8, respectively. When comparing across experiments, note that these significances do not correspond to the same value of the cross section. The *dashed (dotted) black line* is the combination of 13(8) TeV data, requiring the same cross section in both ATLAS and CMS. The *solid black line* is the combined significance of all four data sets

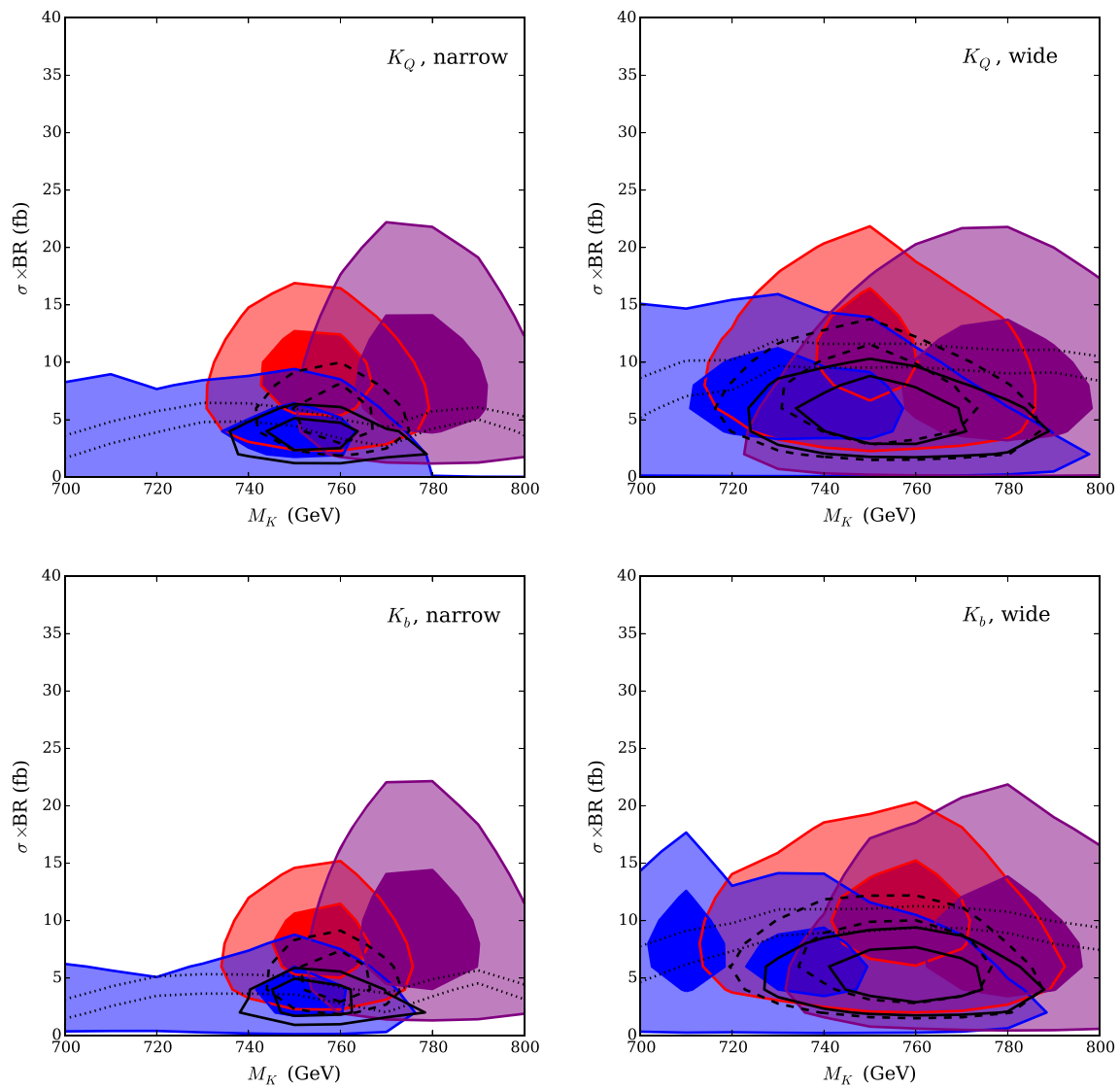


**Fig. 10** Best-fit regions (1 and  $2\sigma$ ) of a spin-2 mediator decaying to diphotons, as a function of mediator mass and 13 TeV cross section, assuming the indicated mediator couplings to partons and mediator width. *Red regions* are the 1 and  $2\sigma$  best-fit regions for the ATLAS13 data, blue is the fit to CMS13 data. The combined best fit for both

ATLAS13 and CMS13 (COMBO13) are the regions outlined in *black dashed lines*. The 1 and  $2\sigma$  upper limits from the combined 8 TeV data (COMBO8) are the *black dashed regions* (with cross sections converted to 13 TeV-equivalents). The best-fit signal combination of all four data sets (COMBO) is the *black solid regions*

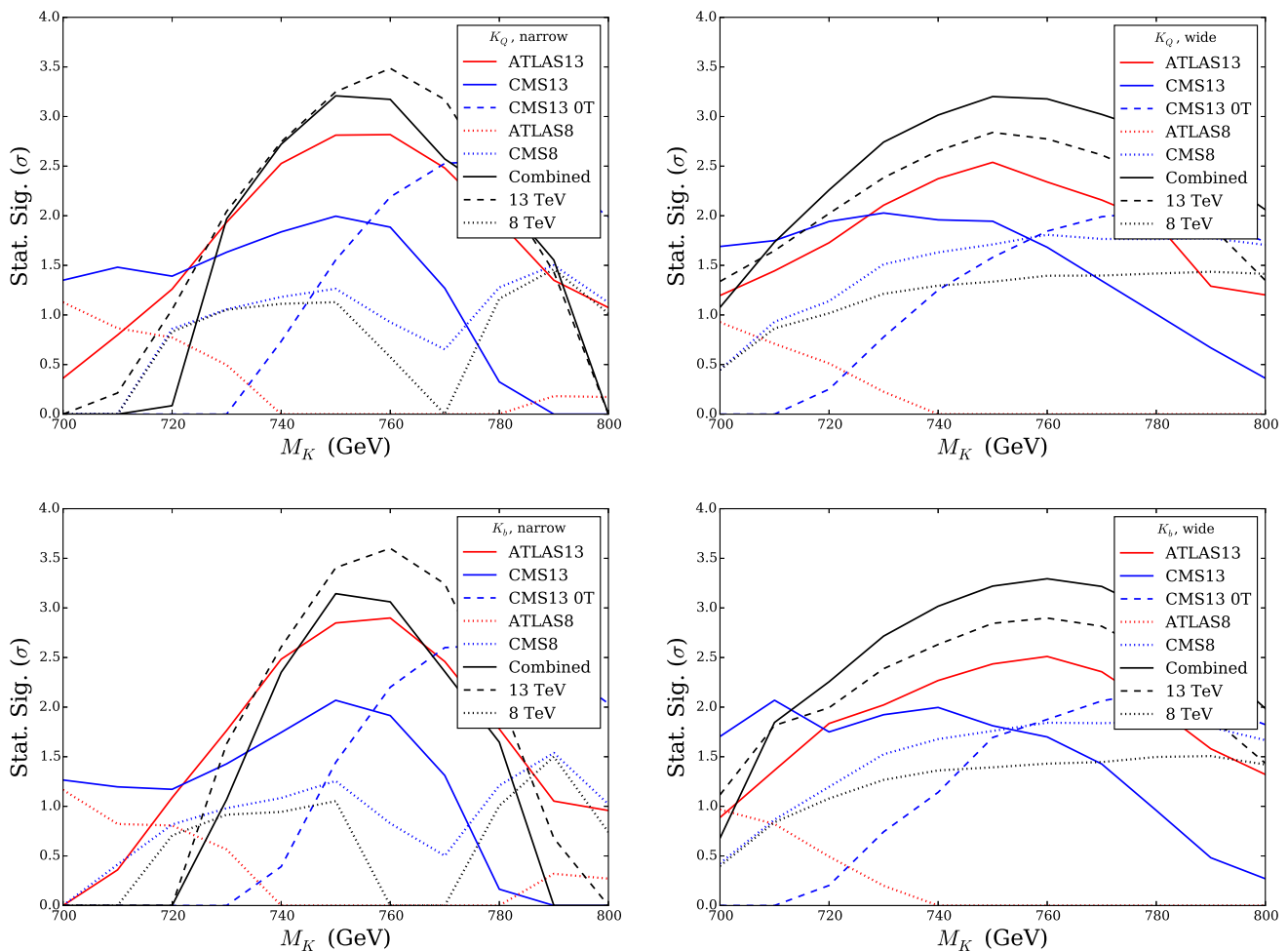


**Fig. 11** Statistical significance for a spin-2 mediator decaying to diphoton, as a function of mediator mass, assuming the indicated mediator couplings to partons and mediator width. At each mass, the cross section is set to the value that maximizes statistical significance for a signal (see Fig. 2). The *solid red line* is the statistical significance of the ATLAS13 data alone, *solid blue* is CMS13, and *dotted red* and

*blue lines* are ATLAS8 and CMS8, respectively. When comparing across experiments, note that these significances do not correspond to the same value of the cross section. The *dashed (dotted) black line* is the combination of 13(8) TeV data, requiring the same cross section in both ATLAS and CMS. The *solid black line* is the combined significance of all four data sets

## References

- ATLAS Collaboration, ATLAS-CONF-2015-081 (2015)
- CMS Collaboration, CMS-PAS-EXO-15-004 (2015)
- N. Craig, P. Draper, C. Kilic, S. Thomas. [arXiv:1512.07733](https://arxiv.org/abs/1512.07733) [hep-ph]
- CMS Collaboration, CMS-PAS-EXO-16-018 (2016)
- ATLAS Collaboration, ATLAS-CONF-2016-018 (2016)
- S. Knapen, T. Melia, M. Papucci, K. Zurek. [arXiv:1512.04928](https://arxiv.org/abs/1512.04928) [hep-ph]
- R.S.Gupta, S. Jger, Y. Kats, G. Perez, E. Stamou, [arXiv:1512.05332](https://arxiv.org/abs/1512.05332) [hep-ph]
- A. Falkowski, O. Slone, T. Volansky. [arXiv:1512.05777](https://arxiv.org/abs/1512.05777) [hep-ph]
- G. Aad et al. [ATLAS Collaboration], Phys. Rev. Lett. **113**(17), 171801 (2014). [arXiv:1407.6583](https://arxiv.org/abs/1407.6583) [hep-ex]
- V. Khachatryan et al. [CMS Collaboration], Phys. Lett. B **750**, 494 (2015). [arXiv:1506.02301](https://arxiv.org/abs/1506.02301) [hep-ex]
- G. Aad et al. [ATLAS Collaboration], Phys. Rev. D **92**(3), 032004 (2015). [arXiv:1504.05511](https://arxiv.org/abs/1504.05511) [hep-ex]
- J.H. Davis, M. Fairbairn, J. Heal, P. Tunney. [arXiv:1601.03153](https://arxiv.org/abs/1601.03153) [hep-ph]
- J. Alwall et al., JHEP **1407**, 079 (2014). doi:[10.1007/JHEP07\(2014\)079](https://doi.org/10.1007/JHEP07(2014)079). [arXiv:1405.0301](https://arxiv.org/abs/1405.0301) [hep-ph]
- T. Sjostrand, S. Mrenna, P.Z. Skands, JHEP **0605**, 026 (2006). [arXiv:hep-ph/0603175](https://arxiv.org/abs/hep-ph/0603175)
- J. de Favereau et al. [DELPHES 3 Collaboration], JHEP **1402**, 057 (2014). [arXiv:1307.6346](https://arxiv.org/abs/1307.6346) [hep-ex]
- M. Chala, M. Duerr, F. Kahlhoefer, K. Schmidt-Hoberg, [arXiv:1512.06833](https://arxiv.org/abs/1512.06833) [hep-ph]
- M. Low, A. Tesi, L.T. Wang. [arXiv:1512.05328](https://arxiv.org/abs/1512.05328) [hep-ph]
- A. Alloul, N.D. Christensen, C. Degrande, C. Duhr, B. Fuks, Comput. Phys. Commun. **185**, 2250 (2014). [arXiv:1310.1921](https://arxiv.org/abs/1310.1921) [hep-ph]
- G. D'Ambrosio, G.F. Giudice, G. Isidori, A. Strumia, Nucl. Phys. B **645**, 155 (2002). [arXiv:hep-ph/0207036](https://arxiv.org/abs/hep-ph/0207036)
- M.R. Buckley, D. Feld, D. Goncalves, Phys. Rev. D **91**, 015017 (2015). [arXiv:1410.6497](https://arxiv.org/abs/1410.6497) [hep-ph]
- P. de Aquino, K. Hagiwara, Q. Li, F. Maltoni, JHEP **1106**, 132 (2011). [arXiv:1101.5499](https://arxiv.org/abs/1101.5499) [hep-ph]

22. G.F. Giudice, R. Rattazzi, J.D. Wells, Nucl. Phys. B **544**, 3 (1999). [arXiv:hep-ph/9811291](#)
23. T. Han, J.D. Lykken, R.J. Zhang, Phys. Rev. D **59**, 105006 (1999). [arXiv:hep-ph/9811350](#)
24. K. Hagiwara, J. Kanzaki, Q. Li, K. Mawatari, Eur. Phys. J. C **56**, 435 (2008). [arXiv:0805.2554](#) [hep-ph]